STEM CELLS TRANSLATIONAL MEDICINE

TISSUE-SPECIFIC PROGENITOR AND STEM CELLS

Human Cartilage-Derived Progenitor Cells From Committed Chondrocytes for Efficient Cartilage Repair and Regeneration

YANGZI JIANG,[a,b,c] YOUZHI CAI,[d,e] WEI ZHANG,[a] ZI YIN,[a] CHANGCHANG HU,[a] TONG TONG,[a] PING LU,[a] SHUFANG ZHANG,[a,b,e] DANTE NECULAI,[a] ROCKY S. TUAN,[c] HONG WEI OUYANG[a,b,d,e,f]

Key Words. Stem and progenitor cells • Chondrocytes • Cartilage repair • Tissue regeneration • Osteoarthritis • Dedifferentiation • Stemness • Stem cell markers • Cell transplantation

[a]Dr. Li Dak Sum & Yip Yio Chin Center for Stem Cell and Regenerative Medicine, [b]Department of Sports Medicine, [d]Department of Orthopaedics, and [f]Collaborative Innovation Center for Diagnosis and Treatment of Infectious Diseases, School of Medicine, Zhejiang University, Hangzhou, People's Republic of China; [c]Center for Cellular Molecular Engineering, Department of Orthopaedic Surgery, University of Pittsburgh School of Medicine, Pittsburgh, Pennsylvania, USA; [e]Chinese Orthopaedic Regenerative Medicine Group, Hangzhou, People's Republic of China

Correspondence: Hong Wei Ouyang, Ph.D., M.D., Center for Stem Cell and Tissue Engineering, School of Medicine, Zhejiang University, Mailbox #39, 388 Yu Hang Tang Road, Hangzhou 310058, People's Republic of China. Telephone: 86-571-88208262; E-Mail: hwoy@zju.edu.cn; or Rocky S. Tuan, Ph.D., Center for Cellular Molecular Engineering, Department of Orthopaedic Surgery, University of Pittsburgh, School of Medicine, 450 Technology Drive, Pittsburgh, Pennsylvania 15219-3143, USA. Telephone: 412-628-2603; E-Mail: rst13@pitt.edu

Received August 7, 2015; accepted for publication February 8, 2016; published Online First on April 29, 2016.

1066-5099/2016/$20.00/0

http://dx.doi.org/10.5966/sctm.2015-0192

ABSTRACT

Articular cartilage is not a physiologically self-renewing tissue. Injury of cartilage often progresses from the articular surface to the subchondral bone, leading to pathogenesis of tissue degenerative diseases, such as osteoarthritis. Therapies to treat cartilage defects using autologous chondrocyte-based tissue engineering have been developed and used for more than 20 years; however, the challenge of chondrocyte expansion in vitro remains. A promising cell source, cartilage stem/progenitor cells (CSPCs), has attracted recent attention. Because their origin and identity are still unclear, the application potential of CSPCs is under active investigation. Here we have captured the emergence of a group of stem/progenitor cells derived from adult human chondrocytes, highlighted by dynamic changes in expression of the mature chondrocyte marker, COL2, and mesenchymal stromal/stem cell (MSC) marker, CD146. These cells are termed chondrocyte-derived progenitor cells (CDPCs). The stem cell-like potency and differentiation status of CDPCs were determined by physical and biochemical cues during culture. A low-density, low-glucose 2-dimensional culture condition (2DLL) was critical for the emergence and proliferation enhancement of CDPCs. CDPCs showed similar phenotype as bone marrow mesenchymal stromal/stem cells but exhibited greater chondrogenic potential. Moreover, the 2DLL-cultured CDPCs proved efficient in cartilage formation both in vitro and in vivo and in repairing large knee cartilage defects (6–13 cm^2) in 15 patients. These findings suggest a phenotype conversion between chondrocytes and CDPCs and provide conditions that promote the conversion. These insights expand our understanding of cartilage biology and may enhance the success of chondrocyte-based therapies. STEM CELLS TRANSLATIONAL MEDICINE *2016;5:733–744*

SIGNIFICANCE

Injury of cartilage, a non-self-repairing tissue, often progresses to pathogenesis of degenerative joint diseases, such as osteoarthritis. Although tissue-derived stem cells have been shown to contribute to tissue renewal and homeostasis, the derivation, biological function, and application potential of stem/progenitor cells found in adult human articular cartilage are incompletely understood. This study reports the derivation of a population of cartilage stem/progenitor cells from fully differentiated chondrocytes under specific culture conditions, which have the potential to reassume their chondrocytic phenotype for efficient cartilage regeneration. These findings support the possibility of using in vitro amplified chondrocyte-derived progenitor cells for joint cartilage repair.

INTRODUCTION

Articular cartilage is a non-self-repairing tissue. Injury of cartilage often marks the initiation of tissue degeneration, and the progressive cartilage loss and subchondral bone sclerosis lead to degenerative joint diseases [1], such as osteoarthritis (OA). Localized articular cartilage defects can be repaired by transplantation of autologous chondrocytes into the injury site, thus slowing disease progress [2, 3] (e.g., chondrocyte-based cell therapies, such as autologous chondrocyte implantation or transplantation and matrix-assisted autologous chondrocyte transplantation [MACT]), were developed and have been used safely in clinical practice [2, 4]. However, uncertainty regarding number and identity of chondrocytes after in vitro expansion remains a major challenge in chondrocyte-based therapies [5]. Search for better cells sources was then warranted.

Tissue-derived stem cells contribute to tissue renewal and homeostasis (e.g., in skeletal muscle, satellite cells contribute to both myofiber repair and stem cell repopulation [6]). There was evidence of self-repair in human articular cartilage, albeit at a low capacity, and cartilage stem/progenitor cells (CSPCs) are thus expected and are currently under investigation (review by Jiang and Tuan [7]). In general, CSPCs were isolated on the basis of their colony-forming ability and identified by virtue of their multilineage differentiation and different surface marker combinations, such as CD105 [8–10], CD166 [8, 9, 11], and STRO-1 [12–14], but their derivation remains unclear.

In the context of developmental origin, multipotent cell subpopulations were found in human embryonic cartilaginous tissue. For example, a CD166(low/−) CD73(−)CD146(+) cell subpopulation was identified in human embryonic limb buds at weeks 5–6 [15]; Quintin et al. also reported that cells possessing chondrogenic, adipogenic, and osteogenic plasticity were found in fetal femurs at weeks 14–16 [16]. However, because of the spatiotemporal inconsistency in their derivations and phenotypes [7], the fate and lineage information of CSPCs are largely unknown.

Several recent studies have demonstrated that parenchymal cells exhibit reserved stemness; for example, in the stomach epithelium, fully differentiated chief cells act as reserve stem cells to generate all epithelial lineages [17], and epithelial cells in the stem cell niche could repopulate the lost stem cells in hair follicles [18]. In vitro culture conditions, including supplements, growth factors, and substrate properties, could also substantially alter cell fate, including cell phenotype and function [19], and pluripotency [20].

In this study, we hypothesized that terminally differentiated human articular chondrocytes possess "reserved stemness" (i.e., stem cell-like potency properties could emerge after culture) and can generate chondrogenic progenitor cells capable of cartilage repair. We report here our observation of the emergence of a group of stem/progenitor cells that were derived from adult human chondrocytes, highlighted by dynamic changes in expression of the mature chondrocyte marker COL2 [21] and the mesenchymal stromal/stem cell (MSC) marker CD146 [21]. These cells are termed chondrocyte-derived progenitor cells (CDPCs). The transition between the stemness and differentiation status of CDPCs was regulated and determined by physical, biochemical, and cell density cues during culture. Specifically, our goal was to probe the emergence and enhancement of these chondrocyte-derived progenitor cells, as well as to evaluate their efficacy on cartilage regeneration both in vitro and in vivo in a clinical study.

MATERIALS AND METHODS

Cell Isolation, Cultivation, Characterization, and Differentiation

The object of our study was to trace the derivation of the adult human cartilage stem cells, the fate decision of their stem cell characteristics, and their effectiveness for cartilage repair. Cells from human adult articular cartilage were isolated and analyzed. Adult articular cartilage samples (47–71 years old; mean, 53.3 years; $n = 51$) were dissected from nonlesion surface areas of the knee joints of patients without signs of rheumatoid involvement undergoing total knee replacement surgery. Patient consent and protocol approval were obtained from the Medical Ethics Committee, Zhejiang University, and from the Institutional Review Board (IRB), University of Pittsburgh and University of Washington. Histological slides of adult healthy articular cartilage tissue ($n = 3$) were donated by the Department of Anatomy, School of Medicine, Zhejiang University. Primary human bone marrow-derived mesenchymal stromal/stem cells (BMSCs) (age 27–46 years, $n = 5$) were isolated with IRB approval from bone marrow and used as a control (details are provided in the supplemental online data). Samples were randomly selected for all analyses; the specific number of biological replicates (i.e., donors) used for each experiment is indicated in the figure legends. Primary chondrocytes were isolated from distal femoral condyles by enzymatic digestion. Briefly, articular cartilage tissue was cut into ~1-mm^3 pieces and digested for 6 hours at 37°C in 0.2% (wt/vol) collagenase (Collagenase Type I, Life Technologies, Thermo Fisher Scientific Life Sciences, Waltham, MA, http://www.thermofisher.com). Cells were transferred to monolayer culture in Dulbecco's modified Eagle's medium (DMEM)/F12 Nutrient Mixture 1:1 (Thermo Fisher Scientific Life Sciences) supplemented with 10% fetal bovine serum (FBS; Thermo Fisher Scientific Life Sciences) and penicillin/streptomycin (50,000 U/50 mg), then cultured under standard conditions. In the glucose concentration study, cells were cultured in DMEM of different glucose concentrations (Life Technologies,Thermo Fisher Scientific Life Sciences). To observe the dynamics of cell phenotype changes, single-cell suspensions were cultured at low density (100–300 cells per cm^2) in low-glucose DMEM containing 10% FBS. Cell proliferation rates were tested in a 2% FBS culture condition and were determined by using Cell Counting Kit-8 (Dojindo, Kumamoto, Japan, http://www.dojindo.com).

Light Microscopy and Immunostaining

Cartilage tissue was fixed in 4% buffered paraformaldehyde and cryosectioned at 14-μm thickness. Cell cultures in 24-well plates were fixed in 4% buffered paraformaldehyde followed by 0.1% Triton X-100 for 30 minutes, washed, and blocked in 1% bovine serum albumin (BSA), then incubated with 200 μl primary antibody diluted 1:50 in phosphate-buffered saline (PBS) at 4°C overnight. After washing, for immunofluorescence, a fluorescently labeled secondary antibody diluted 1:500 was added for 20 minutes at room temperature. Two washing steps with PBS and 4′,6-diamidino-2-phenylindole (Life Technologies, Thermo Fisher Scientific Life Sciences) staining were performed thereafter. For double immunostaining, primary antibodies derived from different species and corresponding, noncross-reacting secondary antibodies were used (information on antibodies is given in the supplemental online data). Cells were examined with an epifluorescence microscope (Olympus X71, Nagano, Japan, http://www.olympus-global.com). For immunohistochemistry, a similar protocol was used except for the use of peroxidase-labeled secondary antibodies followed by diaminobenzidine-based detection.

Flow Cytometry Analysis and Cell Sorting

Cultured cells were detached and incubated with fluorescently labeled antibodies (1×10^6 cells per milliliter, >200 μl/test) at room temperature in the dark, resuspended and washed in PBS, and then pelleted by centrifugation (300*g* for 10 minutes). Isotype-matched IgGs (BD Biosciences, Franklin Lakes, NJ, http://www.bdbiosciences.com) were used as controls, and at least 10,000 live events were analyzed on an FC 500 MCL/MPL Flow Cytometer. Data were evaluated with the aid of CXP Software v2.2 (Beckman Coulter, Sharon Hill, NJ, http://www.beckman.com) (information on antibodies is available in the supplemental online data). For cell cycle test, alcohol-fixed cells were stained with propidium iodide (Life Technologies, Thermo Fisher Scientific Life Sciences). For cell sorting, at least 5×10^6 cells were collected and incubated with fluorescein isothiocyanate-conjugated mouse antihuman CD146 antibody (EMD Millipore, Billerica, MA, http://www.emdmillipore.com/) for 30 minutes at room temperature.

Both CD146(+) and CD146(−) live cell subpopulations were sorted, counted on a Becton Dickinson fluorescence activated cell sorting (FACS) Aria II Flow Cytometer (McGowan Institute, Pittsburgh, PA, http://www.mirm.pitt.edu/), and collected for further study.

Colony Formation Analysis

One hundred cells were seeded in a 10-cm (diameter) dish and cultured with 20% FBS, low-glucose culture medium for the first week. FBS was then reduced to 10%, and the medium was changed every 3 days. After 9–12 days, the cultures were fixed in 1% paraformaldehyde and stained with 1% crystal violet (Sigma-Aldrich, St. Louis, MO, https://www.sigmaaldrich.com/) in methanol for 10 minutes. All cell colonies formed with diameters >2 mm were counted and their size were estimated.

Multilineage Differentiation and Quantification

Osteogenesis, adipogenesis, and chondrogenesis of CDPCs and BMSCs were evaluated (experimental details are provided in the supplemental online data). To generate hyaline three-dimensional (3D) cartilage-like tissue in vitro, 2×10^6 CDPCs were seeded within the insert in a Transwell culture dish (to avoid medium change that disturbs tissue formation) (Corning, Corning, NY, https://www.corning.com) and treated with chondrogenic medium containing transforming growth factor [TGF]-β3 (10 ng/ml, PeproTech, Rocky Hill, NJ, https://www.peprotech.com) and/or bone morphogenetic protein 4 (BMP4, 10 ng/ml; PeproTech, Rocky Hill, NJ) [22, 23]. Samples were collected at week 9 for histological, gene expression, and immunoblot analyses.

Ectopic Implantation of CDPCs in Nude Mice

To test the potential of amplified Col2(−)/CD146(+) CDPCs to generate hyaline cartilage in vivo, 4×10^5 CDPCs at passage 6 were mixed with 0.2 ml fibrin gel (Tisseel, Baxter, Old Toongabbie, NSW, Australia, http://www.baxterhealthcare.com.au) per site and injected subcutaneously into the back of nude mice with six sites per animal (Foxn1nu/Foxn1nu mice, 5 weeks old, female; Jackson Laboratory, Bar Harbor, ME, https://www.jax.org/). All animals were treated according to the standard guidelines approved by Zhejiang University ethics committee (no. ZJU2010101008). After 4 weeks, tissues at the implant sites were harvested and histological sections were stained with hematoxylin and eosin and Safranin O.

Immunoblotting

Proteins were extracted by using radioimmunoprecipitation assay buffer containing protease inhibitors cocktail (Sigma-Aldrich), boiled in SDS-polyacrylamide gel electrophoresis (PAGE) sample buffer (Bio-Rad, Hercules, CA, http://www.bio-rad.com/), and analyzed by SDS-PAGE (6% stacking gel and 12% separating gel). Proteins were blotted onto polyvinylidene fluoride membrane (0.45 μm; EMD Millipore), which was then incubated overnight with the respective primary antibodies (1:1,000; 1% BSA) at 4°C (information on antibodies is given in the supplemental online data). Immunoreactive protein bands were detected after incubation with appropriate secondary antibodies based on ECL signal (GE Healthcare, Chicago, IL, http://www3.gehealthcare.com; Pierce, Thermo Fisher Scientific), and visualized with a FOTO/Analyst1 Fx CCD imaging system (Fotodyne Inc., Hartland, WI, http://www.fotodyne.com/). Results were analyzed with ImageJ 1.45s software (National Institutes of Health, Bethesda, MD, https://imagej.nih.gov/ij/). Gel loading was assessed on the basis of glyceraldehyde-3-phosphate dehydrogenase (GAPDH) immunostaining.

Acellular Cartilage-Derived Matrix

Acellular cartilage matrix (AM) was prepared by using a combination of physical, chemical, and enzymatic treatments [24]. In brief, fresh bovine articular cartilage and meniscus cartilage were minced, frozen, and pulverized in liquid nitrogen with a freezer mill (6870, SPEX SamplePrep, Metuchen, NJ, http://www.spexsampleprep.com/) and the tissue powder was decellularized by Triton X-100 (Sigma-Aldrich) and DNase and RNase (Worthington Biochemical, Lakewood, NJ, http://www.worthington-biochem.com) (additional experimental details are given in the supplemental online data). CDPCs were then mixed with the respective AM powder (5×10^5 cells per 20 mg AM powder in 1 ml of serum-free medium in a 1.5-ml tube) and cultured for 7 days. Relative mRNA expression levels were compared.

mRNA Extraction and Quantitative Reverse Transcription Polymerase Chain Reaction Analysis

Monolayer cultures were extracted by using the RNeasy Mini Kit (Qiagen, Hilden, Germany, https://www.qiagen.com/). 3D cultures were extracted by lysis in Trizol (Thermo Fisher Scientific Life Sciences) followed by treatment with RNase-Free DNase (Qiagen) and fractionated on RNeasy columns. After reverse transcription using random primers (Super Script III First-Strand System, Life Technologies, Thermo Fisher Scientific Life Sciences), quantitative reverse transcription polymerase chain reaction (RT-PCR) was performed (SYBR Green PCR Master Mix, Life Technologies, Thermo Fisher Scientific Life Sciences; StepOne Plus Real-Time PCR system, Applied Biosystems, Thermo Fisher Scientific Life Sciences) and results were calculated using the $2^{-\Delta\Delta Ct}$ method. *18S rRNA, RPL13a,* and *GAPDH* were used as housekeeping genes. The genes, NBI gene ID, primer sequences (5′–3′), and expected amplimer size are listed in the supplemental online data.

Pilot Clinical Study

This study was approved by the Ethics Review Committee of School of Medicine, Zhejiang University, China. The patients were consented for MACT as a two-stage process, with a follow-up arthroscopy procedure including biopsy approximately 1 year after the second stage of the procedure (details are available in the supplemental online data). Magnetic resonance (MR) imaging was performed with a 3.0-T magnet using a knee coil before surgery and at 1 year after surgery. Imaging was performed in the sagittal plane, and a series of T1-weighted and T2-weighted images were obtained as routine sequences. Fat-suppressed three-dimensional fast spoiled gradient-recalled sequences were also performed to obtain additional morphological details, with 1.5-mm slice thickness. MR images were evaluated by two skilled musculoskeletal radiologists. All 15 patients were evaluated using the International Knee Documentation Committee (IKDC) score and Lysholm score before and after surgery. Postsurgical evaluation was carried out a year after surgery. Additional details are provided in the supplemental online data.

Statistical Analysis

Data from at least three independent experiments are reported, and statistical analysis was carried out with data from separate specimens by using SPSS software (version 16.0; IBM, Armonk, NY). Results are presented as mean values and standard deviation (SD) or standard error (SEM). For cell proliferation and CD146 positivity test, after testing for normal distribution and variance homogeneity, a one-way analysis of variance (ANOVA) and post hoc pairwise comparison of mean values were performed, with

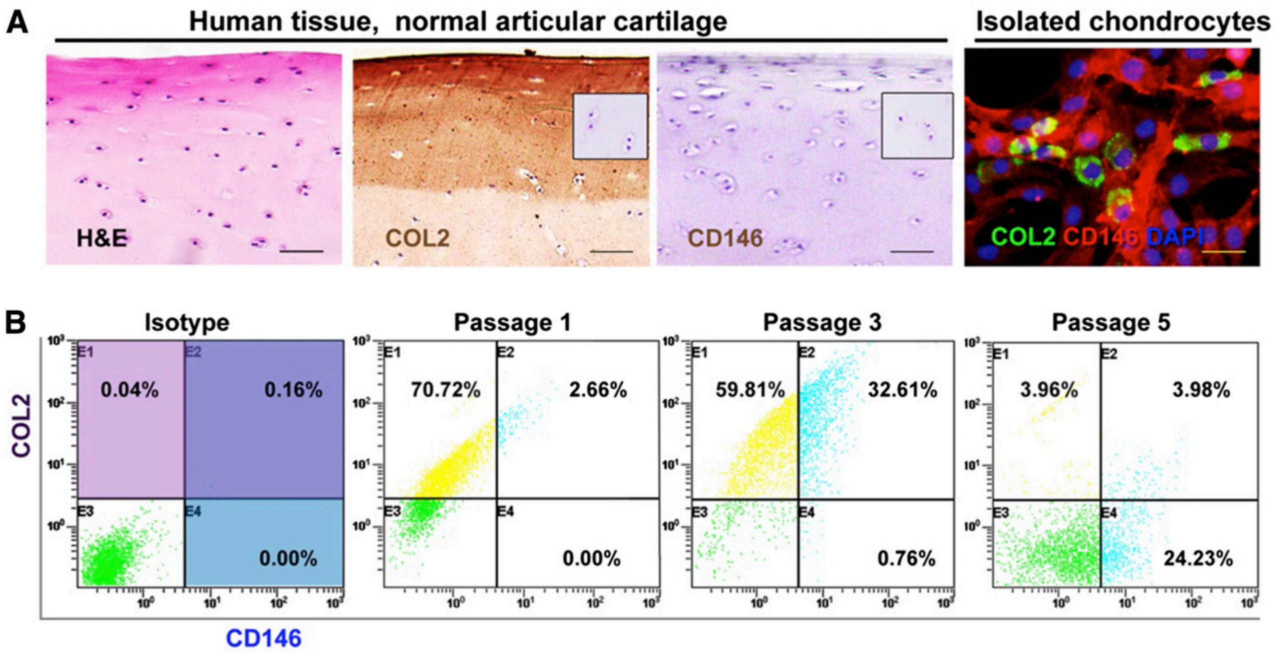

Figure 1. Fully differentiated human chondrocytes change phenotype after isolation. **(A):** COL2 and CD146 immunostaining in healthy articular cartilage from human femoral condyles and isolated chondrocytes. Tissue immunostaining was detected with diaminobenzidine (reddish brown), with hematoxylin nuclear counter stain (bar, 50 μm); passage 4 cell staining was based on immunofluorescence (COL2, green; CD146, red) and DAPI nuclear counterstaining (bar, 20 μm). **(B):** Time course of changes in COL2 and CD146 expression in chondrocytes during monolayer high-density culture and passage. Primary isolated normal human chondrocytes were collected at different passages (P1, P3, and P5), coimmunostained for COL2 and CD146, and analyzed by flow cytometry (n = 3); images were from representative sample. CD146(+) cells are gated in E1 and E2, COL2(+) cells are in E2 and E4, and CD146 and COL2 double-positive cells are in E2. Abbreviations: DAPI, 4′,6-diamidino-2-phenylindole; H&E, hematoxylin and eosin.

statistical significance defined as $p < .05$. For gene expression levels of CD146 in high- and low-density cultures, a two-way ANOVA was performed, with statistical significance defined as $p < .05$. Student's *t* tests were applied to determine statistical significance of differences measured in cell cycle analysis, colony-forming unit (CFU) tests, differentiation quantifications, and clinical scores, with statistical significance defined as $p < .05$.

Results

Articular Cartilage-Derived Chondrocytes Progressively Adopt a Stem/Progenitor Cell-Like Phenotype During Culture In Vitro

We observed that chondrocytes isolated from adult human articular cartilage gradually adopted a stem cell-like phenotype. To profile the dynamics of this phenotype transition, CD146, an early mesenchymal lineage associated surface marker (melanoma cell adhesion molecule), and collagen type II (COL2), a characteristic extracellular matrix component of mature chondrocytes, were used as indicators to trace the kinetics of the emergence of stem cell phenotype from cartilage tissue (Fig. 1). The avascular articular cartilage tissue exhibited a COL2-rich matrix, and it did not harbor any CD146(+) cells (Fig. 1A; supplemental online Fig. 1). When chondrocytes were freshly isolated from healthy cartilage and maintained in high-density, monolayer primary culture condition, the cells gradually became positive for the early-stage MSC marker, CD146 (Fig. 1B). The COL2(+)CD146(−) chondrocytes became COL2(−)CD146(+) cells (Fig. 1B) after a relatively short COL2(+)CD146(+) transition stage, as indicated by the presence of double-immunopositive cells captured by immunofluorescence (Fig. 1A) and flow cytometry (Fig. 1B).

Physical, Biochemical, and Cell Density Culture Regulate Emergence and Proliferation of Stem/Progenitor Cell

A critical culture condition promoted the emergence and maintenance of CD146(+) cells from the articular cartilage-derived cell cultures: seeding at a low cell density (500 cells/cm^2) as monolayer cultures in a low-glucose medium (2DLL culture: monolayer, low density, and low glucose). Low-density seeding reduced cell-cell interactions and allowed cell cycle re-entry (Fig. 2A). Culturing in low-glucose (5.5 mM) medium, generally considered to favor the maintenance of stem cells and to prevent cell aging, resulted in higher proliferation of the cartilage-derived cells, compared with culturing under high glucose (25 mM) (Fig. 2B). Expression levels of genes related to MSC maintenance, self-renewal, and multipotency [25], such as *RAB3B*, Frizzled 7 (*FZD7*), and actin filament-associated protein (*AFAP*), also increased significantly during 2DLL culture (Fig. 2C).

To further characterize the CD146(+) cells, we sorted both CD146(+) and CD146(−) cells from early-passage chondrocyte cultures by FACS and tested their ability to generate CFUs immediately after sorting (Fig. 3B). The CFU activity of CD146(+) cells was significantly higher than that of the CD146(−) cells ($p < .05$), suggesting that CD146(+) cells possessed a stronger self-renewal ability. Interestingly, the CD146(−) cells became CD146(+) (~50%) after 10 additional days of culturing, suggesting the intrinsic potency of the CD146(−) cells.

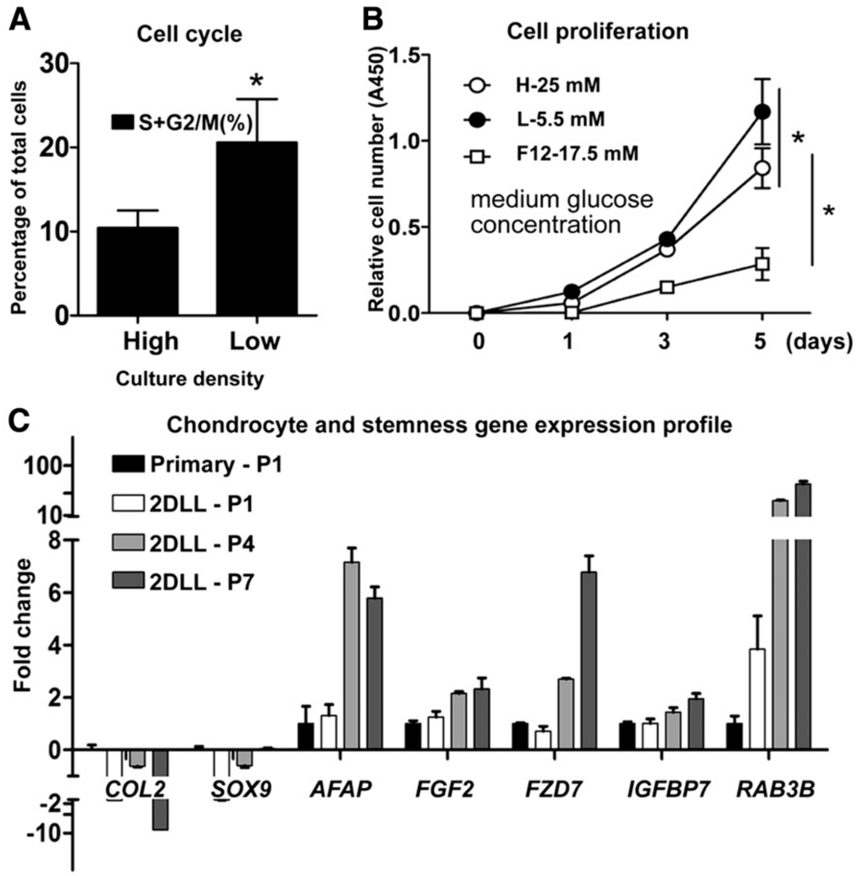

Figure 2. Chondrocytes gain stem cell phenotype under 2DLL culture. **(A):** Cell cycle analysis of high-density (5,000 cells/cm^2, >95% confluence) and low-density (500 cells/cm^2, <50% confluence) cultures determined by flow cytometry. The percentage of cells in active state—S, G2, and M phases—was examined. S+G2/M% = 20.60% ± 5.17% in low-density versus 10.44% ± 2.07% in high-density cultures. Values are mean ± SD (*n* = 5; *, *p* = .007). **(B):** Low-glucose culture enhances chondrocyte-derived progenitor cell proliferation. Data shown from representative sample; values are mean ± SEM (*n* = 5; *, *p* < .05). **(C):** mRNA expression of genes associated with chondrocyte and mesenchymal stromal/stem cell maintenance, self-renewal, and multipotency in primary isolated and high-density cultured chondrocytes and 2DLL-cultured chondrocytes. Results are from representative sample; values (normalized to *RPL13a*) are mean ± SEM (*n* = 3). Abbreviations: 2DLL, 2D monolayer, low density, and low glucose; 2DLL-P1, -4, and -7, different passages of cells under 2DLL culture; F12-17.5 mM: Dulbecco's modified Eagle's medium (DMEM)/F12-1:1, 17.5 mM; G2, gap 2 phase; H-25 mM, high glucose containing DMEM, 25 mM; L-25 mM, low glucose containing DMEM, 5.5 mM; M, mitosis phase; Primary-P1, primary isolated chondrocytes; S, synthesis phase.

Dynamic Transition Between Stem/Progenitor Cell-Like and Chondrocyte Phenotypes

We estimated ~44% CD146(+) cells emerged upon the second passage of 2DLL cultures, with enrichment of the CD146(+) cell population to ~90% after three passages of 2DLL cultures (Fig. 3A). We also found that CD146(+/−) phenotype in chondrocyte-derived cells could be regulated by the in vitro culture environment (Fig. 3). Particularly significant was that the articular cartilage-derived cells were able to transition between a COL2(+)CD146(−) chondrocyte phenotype in 3D culture and a COL2(−)CD146(+) CDPC phenotype in two-dimensional (2D) culture. Thus, when the sorted CD146(+) CDPCs were allowed to condense in a high-density pellet and maintained in TGF-β−containing chondrogenic medium, the CD146 signal was lost and COL2 protein accumulated (Fig. 3B). However, when the cells migrated out from the chondrifying pellets and were subsequently seeded at low density in monolayer culture, the CD146(+) phenotype reappeared (Fig. 3B). Also, chondrocytes seeded at low, noninteractive cell density showed higher *CD146* gene expression during culture (Fig. 3D). These dynamic, coordinated changes strongly suggest that subpopulations of stem/progenitor cells originated from chondrocytes, as a result of their gradual transition to a mesenchymal-like phenotype upon culturing in the absence of cell-cell interactions under monolayer and low-glucose condition (Figs. 2, 3). These cells are termed CDPCs.

Comparison of Multilineage Differentiation Potential of CDPCs and Human Bone Marrow-Derived Mesenchymal Stromal/Stem Cells

To further assess the stem cell characteristics of CDPCs, we compared them with BMSCs with respect to cell surface marker profiles and differentiation multipotency (Fig. 4). Flow cytometry showed that well-recognized MSC-associated surface markers (CD90, CD73, CD105, CD166, CD44, and CD29) were positive in both CDPCs and BMSCs, whereas the hematopoietic stem cell-associated markers (CD34 and CD45) were both negative, indicating similar cell surface epitope profile for CDPCs and BMSCs (Fig. 4A). Both cell types underwent induced differentiation into osteogenic, adipogenic, and chondrogenic lineages (Fig. 4B), although the extent of differentiation was not identical. BMSCs showed higher osteogenic and adipogenic ability than CDPCs, as indicated by stronger alizarin red staining and Oil Red O

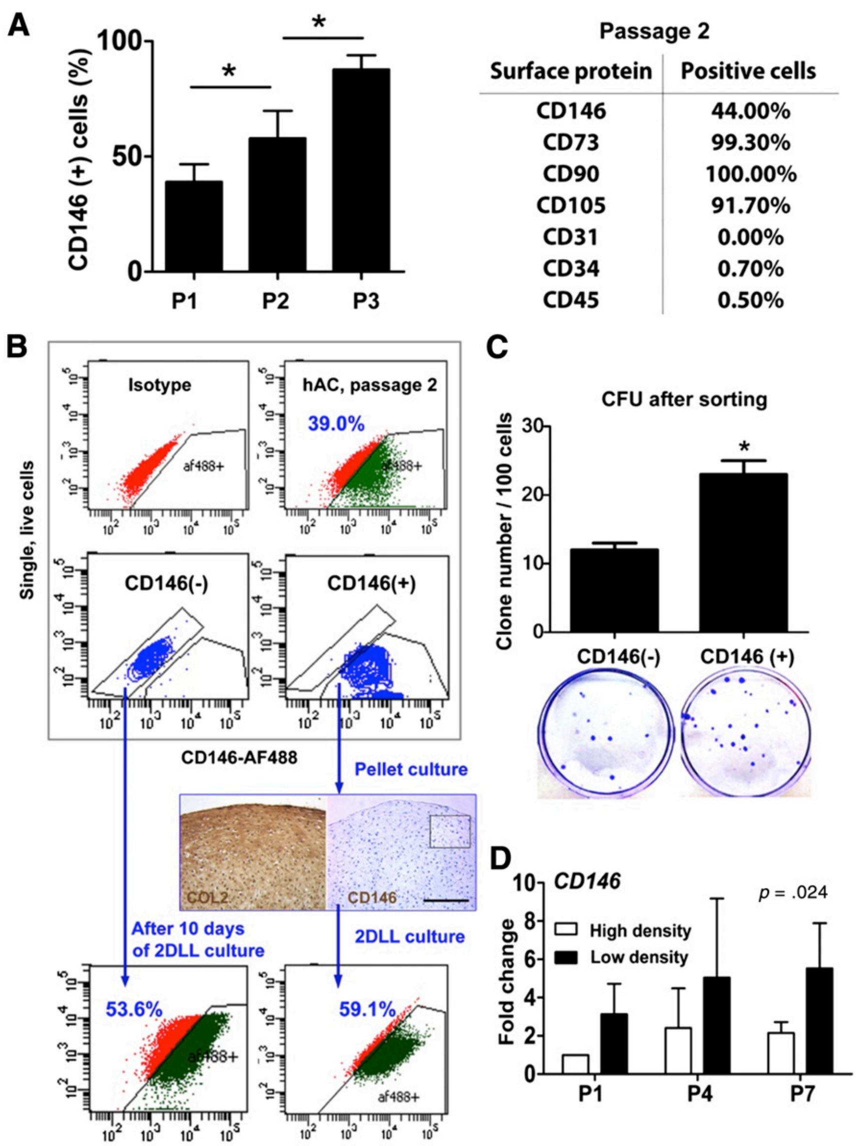

Figure 3. Dynamic CD146(+/−) phenotype change in chondrocyte-derived cells. **(A):** CD146(+) cells increased with passage under 2DLL culture (P1 versus P2: ∗, $p = .017$; P2 versus P3: ∗, $p = .03$; $n = 5$). Values are mean ± SD. Other stem cell surface markers (CD90/CD73/CD105/CD34/CD45/CD31) were also determined by flow cytometry (pooled cells from 5 different donors). **(B):** Cells transitioned between CD146(+)/CD146(−) phenotypes in two-dimensional/three-dimensional cultures of fluorescence activated cell sorted CD146(+) and CD146(−) cells isolated from early-passage human articular chondrocytes (P2; $n = 8$; sorting gate strategy and dynamic change as indicated). High-density pellet (2×10^5 cells) cultures of CD146(+) sorted cells in chondrogenesis medium for 4 weeks stained negative for CD146 (bar, 20 μm). Cells that migrated out from the pellets and placed in 2DLL cultures for a week yielded 59.1% CD146(+) cells, whereas CD146(−) sorted cells cultured for 10 days at low density gave rise to 53.6% CD146(+) cells. **(C):** Colony-forming activity of sorted cells (∗, $p < .05$; values are representative mean ± SEM). **(D):** *CD146* mRNA expression (normalized to *RPL13a*) in high-density and low-density seeded monolayer cultured chondrocytes. Values are mean ± SD (high density versus low density, $p = .024$; $n = 3$). Abbreviations: 2DLL, 2D monolayer, low density, and low glucose; CFU, colony-forming unit; hAC, human articular chondrocytes.

staining, respectively (Fig. 4B). In the pellet chondrogenesis assay, although no significant differences were found in Safranin O histological total scoring, the resulting cell morphologies were different. More fibroblast-like cells were found in BMSCs pellets, whereas more round cells were found in CDPC pellets (Fig. 4B).

Efficient Cartilage Formation With CDPCs In Vitro and In Vivo

To assess whether the high chondrogenic ability of CDPCs can result in the formation of hyaline-like cartilage, CDPCs were placed in 3D cultures in the presence of chondrogenic growth factors. Specifically, 2 million CDPCs were seeded in a Transwell insert and supplemented with the chondro-inductive factors, TGF-β3 and BMP4, which also inhibited hypertrophy in long-term chondrogenic cultures of MSCs and chondrocytes, respectively [22, 23]. After 9 weeks of culture as a condensed cell pellet, a compact, smooth, and translucent structure, which exhibited intense Safranin O staining of matrix sulfated glycosaminoglycans, was obtained (Fig. 5A). The cartilage matrix genes, *COL2* and aggrecan (*AGN*), were expressed at higher levels in the 3D cultures compared with 2D cultured cells, particularly with the addition of

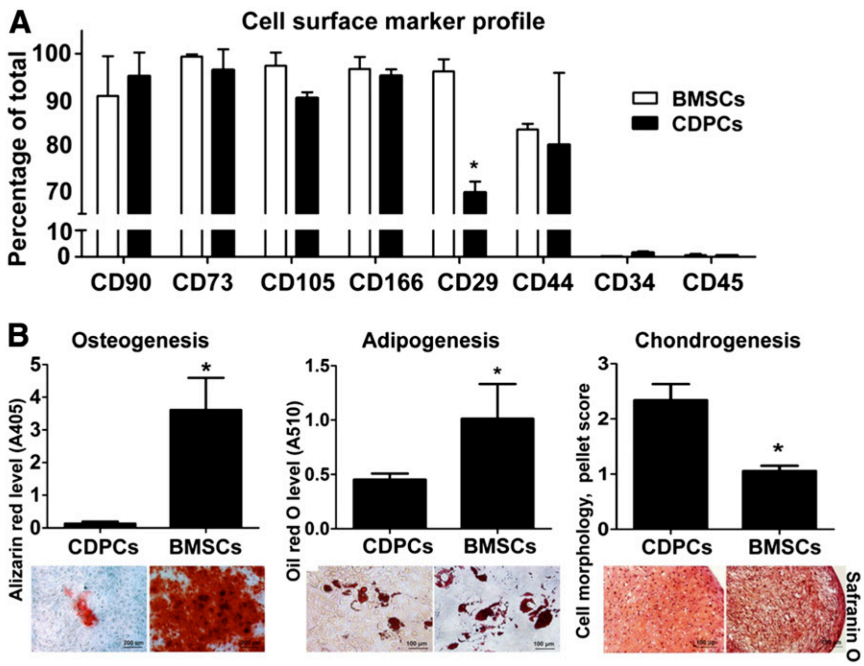

Figure 4. Stem cell characteristics of CDPCs versus BMSCs. **(A):** Cell surface epitope profiles analyzed by flow cytometry. CD90/73/105/166/29/44/34/45 were tested in CDPCs and BMSCs (values are mean ± SD; $n = 5$ each; *, $p = .004$). **(B):** Osteogenic, adipogenic, and chondrogenic differentiation potential of human CDPCs and human BMSCs. **(B, left):** Alizarin red staining (bar, 200 μm) represented the osteogenic potential and was quantified (values are mean ± SD; $n = 3$ each; *, $p = 2.17 \times 10^{-6}$). **(B, middle):** Oil Red O staining (bar, 100 μm) represented adipogenic potential and was quantified (values are mean ± SD; $n = 3$ each; *, $p = .009$). **(B, right):** Safranin O staining (bar, 100 μm) represented chondrogenic potential and was quantified by pellet score (values are mean ± SD; $n = 3$ each; *, $p = .004$). Abbreviations: BMSC, bone marrow-derived stem cell; CDPC, chondrocyte-derived progenitor cell.

BMP4, with detectable activation of signaling via the downstream targets of BMPs, the SMA (small body size)- and MAD (mothers against decapentaplegic)-related proteins (SMADs) (increased pSMAD2, decreased pSMAD1, 5) (Fig. 5A).

To assess the potential application of their intrinsic chondrogenic ability for cartilage repair, CDPCs were seeded directly and cultured within AMs [26] prepared from bovine joint surface cartilage (hyaline cartilage) and meniscus (fibrocartilage) to mimic host tissue environments in vivo upon CDPC transplantation. *COL2*, *AGN*, and *SOX9* gene expression by CDPCs increased significantly upon seeding and culture within hyaline cartilage-derived AM, whereas only the *SOX9* gene was upregulated in the meniscus-derived AM (Fig. 5B); this finding suggests that exposure to a native cartilage matrix environment was capable of enhancing the expression of the innate chondrogenic potential of CDPCs, without exogenous stimulation with chondrogenic factors.

The ability of CDPCs to form hyaline cartilage in vivo was next tested by subcutaneous injection of 0.4 million CDPCs in 0.2 ml fibrin gel into the backs of immunodeficient mice. After 4 weeks, histologically hyaline cartilage-like tissues were formed in 4 of 6 injection sites, displaying round cells sited in lacunae surrounded by Safranin O-positive matrix (Fig. 4C). Taken together, these in vitro and in vivo observations strongly suggest cartilage regenerative potential of CDPCs.

Clinical Repair of Large Cartilage Defects With CDPCs

A pilot clinical study was designed to evaluate the feasibility of the therapeutic application of CDPCs. Only knee joints without other concomitant joint problems, such as OA inflammation, are considered eligible as the host tissue for CDPC transplantation. Thus, confounding variables, such as proinflammatory cytokines [27] that could act to inhibit matrix production, or induce matrix degeneration [28], and cell apoptosis [29], are eliminated. Patients without inflammatory lesion and joint instability, with a cartilage defect more than 6 cm^2 in size, were enrolled in the prospective pilot study. Fifteen patients (2 female and 13 male patients) with a mean age of 25.0 years (range, 16–36 years) were treated with CDPCs in a matrix-assisted cell transplantation procedure. The sites of the defects were as follows: medial femoral condyle ($n = 9$), lateral femoral condyle ($n = 5$), and medial femoral condyle extending to trochlear groove ($n = 1$). The average size of the defects was 8.5 cm^2 (range, 6–13 cm^2) and the defects were classified as grade III and IV according to International Cartilage Repair Society criteria (supplemental online Table 1).

After a standard diagnostic procedure, full-thickness cartilage specimens (200–300 mg) were harvested with a sharp gouge from a non-weight-bearing area of the trochlear ridge or intercondylar notch under arthroscopy. Chondrocytes were isolated from the cartilage specimen and culture-expanded to the desired cell number under Good Manufacturing Practice conditions. After 2–3 weeks of 2DLL culture in vitro, the CDPCs were seeded in a collagen type I/III scaffold to form the cartilage implant and then surgically implanted into the cartilage defects (additional details of the clinical procedure are available in the supplemental online data).

Clinical Scores

The clinical scores indicated satisfactory maintenance of the loading capacity of the treated knee joint short term, as well as stable clinical improvement. Clinical evaluation showed significant improvement on the basis of IKDC scores (from 60.1 ± 15.4 before

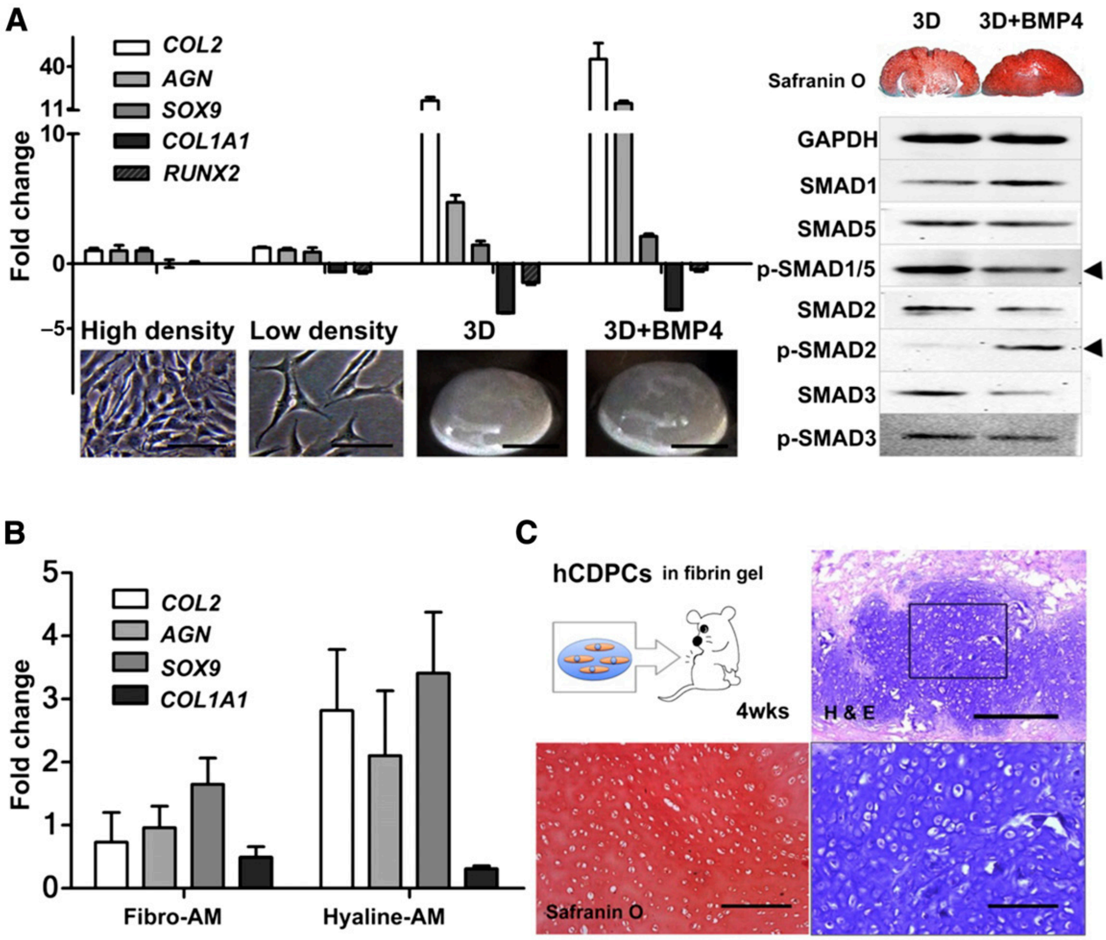

Figure 5. Cartilage-forming ability of CDPCs in vitro and in vivo. **(A)**: CDPCs generated hyaline cartilage-like tissue in vitro. Gene expression was analyzed in monolayer cultures (high density, >95% confluence; low density, <50% confluence), and in 3D cultures consisting of 2×10^6 CDPCs in transforming growth factor-β3 (10 ng/ml) containing chondrogenic medium, with or without BMP4 (10 ng/ml), for 9 weeks. Cell morphology of two-dimensional cultures (bar, 50 μm), and Safranin O staining and gross morphology in 3D cultures (bar, 3 mm) are shown. Western blot analysis showed SMAD signaling response to BMP4 stimulation in 3D cultures. **(B):** CDPCs (5×10^5 cells) seeded in AM (20 mg dry weight), extracted from healthy bovine articular cartilage (hyaline) and meniscus (fibro) and cultured in serum-free medium for 7 days. Relative mRNA expression levels of *COL2*, *AGN*, *SOX9*, and *COL1* (normalized to *RPL13a*) were compared. Values from pooled samples are mean ± SEM (*n* = 6). **(C):** CDPCs (4×10^5 cells in 0.2 ml fibrin gel) injected subcutaneously into nude mice generated hyaline cartilage-like tissue in vivo, analyzed at 4 weeks after surgery. **(C, right):** H&E staining: bar, 100 μm (top) and 50 μm (bottom). **(C, left):** Safranin O staining (bar, 100 μm). Abbreviations: 3D, three-dimensional; AM, acellular cartilage matrix; BMP4, bone morphogenetic protein 4; GAPDH, glyceraldehyde-3-phosphate dehydrogenase; H&E, hematoxylin and eosin; hCDPC, human chondrocyte-derived progenitor cell; SMAD, SMA (small body size)- and MAD (mothers against decapentaplegic)-related proteins.

surgery to 91.6 ± 4.3 at 12 months after surgery; $p < .05$) and Lysholm score (from 52.1 ± 15.1 to 89.3 ± 5.5; $p < .05$) after the CDPC-based procedure.

MRI Evaluation

All patients were followed prospectively after CSPC implantation, and the repair tissue site was graded as completely attached, partially attached, or detached. In all 15 patients, completely attached grafts were found (Fig. 6A; supplemental online Table 2). The cartilage defect site was totally covered by the implanted repair tissue, which showed equivalent intensity compared with the surrounding cartilage in 13 patients and lower intensity in the remaining two patients. The contour of the subchondral bone was smooth and regular in 14 patients and irregular in 1 patient. Tissue hypertrophy and infection have been reported to be the most common adverse events of cell-based cartilage repair, and a second intervention was often required after graft failure [30]; in our study, we did not observe any postoperative complications (*n* = 0).

Histology

Postoperative second-look arthroscopy (Fig. 6A) was performed on four patients. In all four patients, the grafted area appeared to be matrix-rich, with well-preserved hyaline-like cartilage architecture. Histological examination of biopsy samples from the 4 patients showed that compared with the adjacent arthritic cartilage, the repair tissue demonstrated the presence of chondrocyte-like cells and hyaline cartilage-like structure and matrix (i.e., COL2[+], COL1[−], and COL10[−]) (Fig. 6B). All four biopsy specimens were free of ectopic calcification and vascularization. No evidence of inflammation was observed.

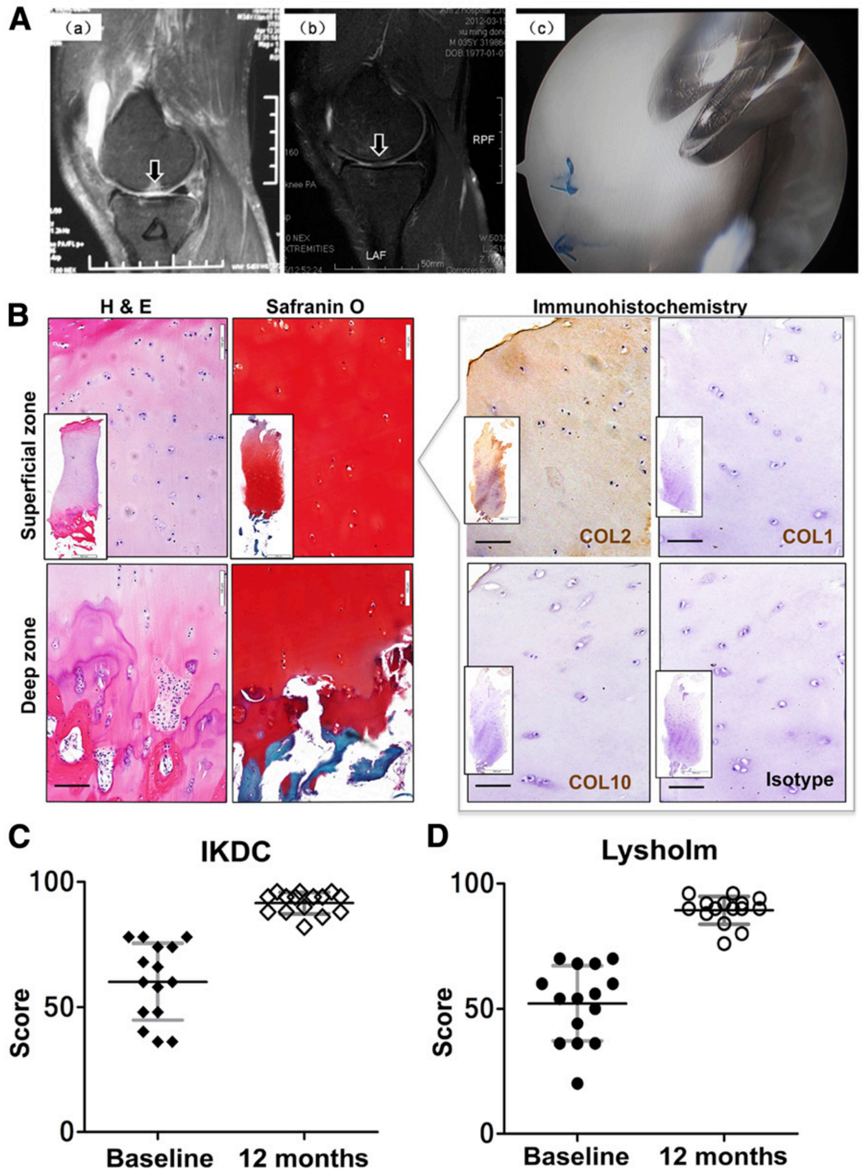

Figure 6. Articular cartilage repair by CDPCs transplanted in patients with large size (>6 cm^2) cartilage defects. **(A):** Representative magnetic resonance imaging (MRI) and arthroscopy images to assess cartilage repair. **(A, a):** Preoperative MRI/sagittal oblique imaging of femoral condyle with cartilage defect. **(A, b):** MRI of repaired cartilage 12 months after chondrocyte-derived progenitor cell (CDPC) transplantation. Complete attachment and filling of the defect are shown (arrows indicate the transplanted areas). **(A, c):** Second-look arthroscopy 12 months after CDPC transplantation. **(B)**: Histological analysis of repaired tissue, 12 months after CDPC transplantation. Insets show low-magnification structural overview of cylinder harvested with bio-punch (bar, 500 μm). High-magnification micrographs show the superficial zone and deep zone of repaired cartilage in the repair tissue. **(B, left):** H&E staining (bar, 100 μm); (Safranin O staining (bar, 100 μm). **(B, right):** Immunohistochemistry of COL2, COL1, and COL10 for repaired cartilage. Tissue immunostaining was detected with diaminobenzidine (reddish brown), with hematoxylin nuclear counterstain (bar, 100 μm). **(C):** Clinical scoring evaluations of IKDC score. Each data point represents one patient, compared with preoperative situation (n = 15; $p = 1.43 \times 10^{-6}$). **(D):** Clinical scoring evaluations of Lysholm score. Each data point represents one patient, compared with preoperative situation (n = 15; $p = 1.04 \times 10^{-7}$). Abbreviations: H&E, hematoxylin and eosin; IKDC, International Knee Documentation Committee.

Pain and Functional Evaluation

As indicated earlier, the IKDC and Lysholm scores from questionnaires regarding pain, swelling, blockage of knee, and general condition of the knee suggested generally favorable outcomes. All patients had scored poorly before the operations. One year after CDPC-based MACT, all patients had reduced knee pain and swelling, and locking sensation had disappeared (supplemental online Table 2). In all 15 patients, the mean IKDC score increased from 60.1 to 91.6 1 year after surgery (Fig. 6C), demonstrating a significant improvement ($p < .05$) compared with the preoperative findings. Concomitantly, the Lysholm score improved from 52.1 to 89.3 ($p < .05$) (Fig. 6D). Fourteen patients returned to normal daily living and sports activities within 1 year after treatment.

Discussion

Although autologous chondrocyte-based therapies have been in use for more than 20 years [2, 4], the challenge of in vitro chondrocyte expansion remains. A promising cell source, CSPCs, has recently attracted considerable attention, and their origin and identity are being investigated.

In this study, the emergence of the stem/progenitor cell phenotype from chondrocytes was for the first time captured kinetically by profiling the expression of the chondrocyte marker COL2 and a MSC marker, CD146. Our results strongly suggest that fully differentiated chondrocytes possess "reserved stemness," which is reactivated during in vitro expansion, gradually displaying multipotent stem/progenitor cell characteristics. We have termed these cells as chondrocyte-derived progenitor cells (CDPCs) and have shown that their stem and differentiation status is regulated as a function of their placement in low-density 2D versus high-density 3D cultures. We then demonstrated that the amplified CDPCs are capable of functional cartilage repair both in vitro and in a clinical study on patients with large articular cartilage defects (6–13 cm^2). The reversible phenotype transition between chondrocytes and progenitor cells reported here provides information on the origin of human articular cartilage stem/progenitor cells and brings new insights into cartilage biology and the development of chondrocyte-based therapies.

To trace the origin of CSPCs, a mature chondrocyte-associated marker, COL2 [21], and an early mesenchymal lineage surface marker, CD146 [21, 31, 32], were used to profile the kinetics of the emergence of CSPCs from cartilage tissue. The avascular articular cartilage tissue exhibits COL2-rich matrix but does not harbor any CD146(+) cells, which are generally considered to be primarily located at perivascular sites [31]. Once placed in monolayer culture, primary chondrocytes are known to dedifferentiate [33] and to become fibroblast-like and lose their chondrocytic phenotype (i.e., COL2[−]) [34]. Here we observed that chondrocytes gradually express CD146, an early-stage MSC marker during in vitro culture (Fig. 1). The conversion of COL2(+) CD146(−) chondrocytes to the COL2(−)CD146(+) mesenchymal progenitor-like phenotype is marked with a short transitional state of COL2(+)CD146(+) phenotype, detected as double-immunopositive cells by immunofluorescence and flow cytometry.

We observed that low cell density, monolayer culture in a low-glucose medium (2DLL culture) greatly promoted the emergence and maintenance of CD146(+) cells. Consistent with the reported promotion of stem cell maintenance [35] and prevention of cell aging [36] in low-glucose cultures, we also observed higher cell proliferation in low-glucose cultures (5.5 mM) than in high-glucose cultures (25 mM). Upon 2DLL culture, approximately 40% of cells were CD146(+) after first passage, and this population was enriched to ~90% after three passages (Fig. 3). In addition, higher cell cycle re-entry was seen in cultures seeded at low density (Fig. 2), concomitant with higher *CD146* gene expression (Fig. 3D). Analysis of CFU activity of FACS-sorted CD146(+) and CD146(−) cells from early-passage chondrocytes (Fig. 3B) showed that the former consistently produced more clonal colonies (Fig. 3C). Interestingly, the CD146(−) cells appeared to transition to CD146(+) cells (~50%) after 10 additional days of 2DLL culturing, suggesting that the time-dependent emergence of CD146(+) cells in the primary culture was likely the result of both the proliferation of CD146(+) cells and change in phenotype of the originally CD146(−) cells (Fig. 3B).

We also found that these chondrocyte-derived CD146(+) cells exhibited the phenotype of mesenchymal stem/progenitor cells: (a) They displayed similar stem cell surface markers as bone marrow-derived/stromal cells (Figs. 3A, 4A); (b) they could be induced to undergo osteo-, adipo- and chondrogenesis (Fig. 4B); (c) they showed higher CFU activity than CD146(−) cells (Fig. 3C); and (d) they could form cartilage tissue both in vitro and in vivo (Figs. 4, 5). Besides the changes in COL2/CD146 expression, additional evidence supporting the chondrocyte-stem/progenitor phenotypic transition is also noted during the in vitro 2DLL expansion, including (a) the upregulation of expression of stem cell-related multipotency genes [25], such as *RAB3B*, *FZD7*, and *AFAP* (Fig. 2C); (b) cell-cycle re-entry (Fig. 2A); and (c) expression of MSC-related cell surface markers after 2 passages of 2DLL cultures, although not synchronized with CD146 expression (Fig. 3A). Taken together, these dynamic, coordinated changes support the notion that the CDPCs originate from chondrocytes, which gradually change to mesenchymal-like cells upon culturing under minimized cell-cell interaction conditions.

The concept of "dedifferentiation" has different meanings in the context of stem cell/developmental biology compared with chondrocyte biology [33, 37]. In stem cell biology, dedifferentiation describes the reverse developmental process in which differentiated cells with specialized functions become undifferentiated progenitor cells. Dedifferentiation and subsequent proliferation thus provide the basis for tissue regeneration and the formation of new stem cell lineages [37]. In chondrocyte biology, the phenotype shifting of chondrocytes to a fibroblast-like state when cultured in monolayers was referred to as "dedifferentiation" [5, 33]. In this process, cells underwent morphological changes and stopped producing a cartilage-specific matrix, but regression to an earlier biopotent or multipotent state was not implied [33]. Interestingly, Tallheden et al. [38] reported that some of the culture-expanded normal human articular chondrocytes demonstrated multipotency [38]. Therefore, the exact mechanisms underlying the reversibility of this process are unknown and deserve further investigation.

Our finding of the emergence of stem cell phenotype from chondrocytes presents a biological scenario distinct from the conventional unidirectional stem cell hierarchies (i.e., that a population of mature chondrocytes possesses intrinsic "stemness," which could reverse into progenitor stage during in vitro culture expansion). This observation supports an alternative cellular feature that mature, differentiated cells are able to revert to a stem/progenitor cell stage and contribute to tissue regeneration. Of relevance is a recent study on fully differentiated chief cells of the stomach epithelium that act as reserve stem cells to generate cells of all lineages [17].

Studies on adult tissue-specific stem cells have suggested that they are likely present as a stem/progenitor cell population that is kept quiescent and is activated when needed, and may be identified and traced with a specific cell marker from early stages of development; examples include muscle satellite cells [6] and hematopoietic stem cells [39]. Wu et al. identified a CD166(low/−) CD73(−)CD146(+) cell subpopulation in human embryonic limb buds at weeks 5–6 and showed that the CD146(+) phenotype disappeared in 8-week embryo [15]. We also were unable to detect any CD146(+) cells in adult human articular cartilage in vivo. Therefore, it is still unclear whether CSPCs are quiescent stem cell that are left from earlier development, remain reserved in tissue, and then become reactivated upon in vitro culture or instead whether most mature chondrocytes have such potential to become progenitors. A more in-depth analysis of the stem/progenitor cell populations in a future study is needed.

We next investigated the extrinsic factors that can regulate the transition between chondrocytes and stem/progenitor cells. We found that cells are able to change between COL2(+)CD146(−) chondrocyte phenotype in 3D culture and COL2(−)CD146(+) CDPC phenotype in 2D culture (Figs. 1, 3A). When the sorted CD146(+) cells were condensed to form a chondrogenic pellet, the CD146 signal was lost and accumulation of COL2 protein was seen (Fig. 3B); interestingly, CD146(+) cells reappeared when the cells migrated out from the chondrifying pellets and maintained their CD146(+) phenotype when subsequently seeded at low density in monolayer culture (Fig. 3B). These observations point toward the bidirectional nature of cell lineage commitment to adopt new fates in a manner regulated by different host microenvironments. The functional extent of this phenotype transition was further tested both in vitro and in vivo. We cultured CDPCs in native acellular matrices of different cartilage environment, derived from hyaline- and fibro-cartilage tissues [26] and observed that the former more favorably promoted CDPC chondrogenesis than did the latter (Fig. 5B). Upon ectopic implantation in immunodeficient mice in vivo, CDPCs produced robust cartilage tissue without the addition of any chondrogenic growth factors (Fig. 5C), indicating that the CDPCs are capable of forming cartilage.

Taken together, these results support the potential application of CDPCs for the repair of cartilage defects. Specifically, CDPCs are intrinsically highly chondrogenic, and the host hyaline cartilage tissue matrix may support chondrogenesis of the implanted cells. Thus, CDPCs may be used to form neo-cartilage in a cartilage defect without extrinsic inductive influences.

We therefore initiated a pilot clinical study to evaluate the application of CDPCs in cell therapy for cartilage repair using a standard MACT procedure. The 2DLL-cultured CDPCs showed efficacy in the repair of large knee cartilage defects (defect size, 6–13 cm^2) in all 15 patients tested. The results reported here, including subjective and objective evaluations, are highly promising. By the first 6 months of follow-up, patients were able to do light work or sports; after 1 year, none of the patients showed moderate or severe limitation in daily activities, such as walking or climbing stairs. All patients were satisfied with their clinical outcomes and reported good quality of life. Both IKDC and Lysholm scores improved significantly at 1 year after surgery. The clinical and functional results of this study are similar or superior to those previously reported in patients who underwent other chondrocyte-based implantation procedures [30, 40], with no increased risk for complications during the first year of follow-up. We note that a previous report showing that CSPCs derived from OA cartilage populate diseased tissue in vitro [41]. In our study, we have a strictly controlled cell source and host environment (i.e., the CDPCs used were derived from healthy cartilage and were placed in defects of joints without observable OA-associated inflammation). As such, confounding variables such as proinflammatory cytokines [27] that could act to inhibit matrix production, or induce matrix degeneration [28] and cell apoptosis [29] are eliminated. As far as the enrollment in the clinical study is concerned, only 15 young patients were included; further evaluations in older patients, as well as a larger patient population with longer-term follow-ups, are clearly needed.

Conclusion

We report here that a population of cartilage stem/progenitor cells can be derived from fully differentiated chondrocytes that have the potential to reassume their chondrocytic phenotype for efficient cartilage regeneration. This novel concept supports the possibility of using in vitro amplified chondrocyte-derived cells, the CDPCs, for joint repair. Importantly, it provides an alternative view to the widely accepted model that dedifferentiated chondrocytes are merely fibroblastic cells with minimal tissue regenerative ability. These findings strongly suggest that identification of the extrinsic influences that determine the fate of CDPCs is of great value in manipulating CDPCs for their therapeutic applications for cartilage repair.

Acknowledgments

We thank Drs. Shi Peihua, Shen Weiliang, and Zou Xiaohui (Zhejiang University) for tissue collection; Lynda Guzik (McGowan Institute for Regenerative Medicine) for FACS; and Dr. Paul Manner (University of Washington) for human tissues. This research was supported by (a) Zhejiang University: National Key Scientific Program (2012CB966604), the National High Technology Research and Development Program of China (863 Program) (2012AA020503, 2015AA020302, 2015AA020303), National Natural Science Foundation of China grants (81125014, 81330041, 81472115, 81101356, 81201395, J1103603, 31000436), Key Scientific and Technological Innovation Team of Zhejiang Province (2013TD11), Zhejiang Provincial Grants (LY13C100001, 2012C3112, 2012C33015), and sponsorship by the Regenerative Medicine in Innovative Medical Subjects of Zhejiang Province and Zhejiang Provincial Program for the Cultivation of High-level Innovative Health Talents, and (b) University of Pittsburgh: Commonwealth of Pennsylvania Department of Health (SAP 4100050913), U.S. Department of Defense (W81XWH-08-2-0032, W81XWH-10-1-0850, W81XWH-14-2-0003, and W81XWH-14-1-0217), and National Institutes of Health (1U18TR000532).

Author Contributions

Y.J.: conception and design, administrative support, collection and/or assembly of data, data analysis and interpretation, manuscript writing, final approval of manuscript; Y.C.: provision of study material or patients, collection and/or assembly of data, data analysis and interpretation, final approval of manuscript; W.Z., C.H., and T.T.: collection and/or assembly of data, data analysis and interpretation, final approval of manuscript; Z.Y.: conception and design, collection and/or assembly of data, data analysis and interpretation, final approval of manuscript; P.L. and S.Z.: conception and design, data analysis and interpretation, manuscript writing, final approval of manuscript; D.N.: data analysis and interpretation, manuscript writing, final approval of manuscript; R.S.T.: financial support, administrative support, experimental conception and design, provision of study material or patients, data analysis and interpretation, manuscript writing, final approval of manuscript; H.W.O.: conception and design, financial support, administrative support, provision of study material or patients, experimental conception and design, collection and/or assembly of data, data analysis and interpretation, manuscript writing, final approval of manuscript.

Disclosures of Potential Conflicts of Interest

The authors indicated no potential conflicts of interest.

References

1 Moskowitz RW. Osteoarthritis: Diagnosis and Medical/Surgical Management. Baltimore, MD: Wolters Kluwer Health/Lippincott Williams & Wilkins, 2007.

2 Brittberg M, Lindahl A, Nilsson A et al. Treatment of deep cartilage defects in the knee with autologous chondrocyte transplantation. N Engl J Med 1994;331:889–895.

3 Jiang YZ, Zhang SF, Qi YY et al. Cell transplantation for articular cartilage defects: Principles of past, present, and future practice. Cell Transplant 2011;20:593–607.

4 Peterson L, Vasiliadis HS, Brittberg M et al. Autologous chondrocyte implantation: A long-term follow-up. Am J Sports Med 2010;38:1117–1124.

5 Schnabel M, Marlovits S, Eckhoff G et al. Dedifferentiation-associated changes in morphology and gene expression in primary human articular chondrocytes in cell culture. Osteoarthritis Cartilage 2002;10:62–70.

6 Brack AS, Rando TA. Tissue-specific stem cells: Lessons from the skeletal muscle satellite cell. Cell Stem Cell 2012;10:504–514.

7 Jiang Y, Tuan RS. Origin and function of cartilage stem/progenitor cells in osteoarthritis. Nat Rev Rheumatol 2015;11:206–212.

8 Pretzel D, Linss S, Rochler S et al. Relative percentage and zonal distribution of mesenchymal progenitor cells in human osteoarthritic and normal cartilage. Arthritis Res Ther 2011;13:R64.

9 Alsalameh S, Amin R, Gemba T et al. Identification of mesenchymal progenitor cells in normal and osteoarthritic human articular cartilage. Arthritis Rheum 2004;50:1522–1532.

10 Bernstein P, Sperling I, Corbeil D et al. Progenitor cells from cartilage–no osteoarthritis-grade-specific differences in stem cell marker expression. Biotechnol Prog 2013;29:206–212.

11 Fickert S, Fiedler J, Brenner RE. Identification of subpopulations with characteristics of mesenchymal progenitor cells from human osteoarthritic cartilage using triple staining for cell surface markers. Arthritis Res Ther 2004;6:R422–R432.

12 Grogan SP, Miyaki S, Asahara H et al. Mesenchymal progenitor cell markers in human articular cartilage: normal distribution and changes in osteoarthritis. Arthritis Res Ther 2009;11:R85.

13 Karlsson C, Lindahl A. Articular cartilage stem cell signalling. Arthritis Res Ther 2009;11:121.

14 Otsuki S, Grogan SP, Miyaki S et al. Tissue neogenesis and STRO-1 expression in immature and mature articular cartilage. J Orthop Res 2010;28:96–102.

15 Wu L, Bluguermann C, Kyupelyan L et al. Human developmental chondrogenesis as a basis for engineering chondrocytes from pluripotent stem cells. Stem Cell Rep 2013;1:575–589.

16 Quintin A, Schizas C, Scaletta C et al. Plasticity of fetal cartilaginous cells. Cell Transplant 2010;19:1349–1357.

17 Stange DE, Koo BK, Huch M et al. Differentiated Troy+ chief cells act as reserve stem cells to generate all lineages of the stomach epithelium. Cell 2013;155:357–368.

18 Rompolas P, Mesa KR, Greco V. Spatial organization within a niche as a determinant of stem-cell fate. Nature 2013;502:513–518.

19 Gilbert PM, Havenstrite KL, Magnusson KE et al. Substrate elasticity regulates skeletal muscle stem cell self-renewal in culture. Science 2010;329:1078–1081.

20 Hou P, Li Y, Zhang X et al. Pluripotent stem cells induced from mouse somatic cells by small-molecule compounds. Science 2013;341:651–654.

21 Halfon S, Abramov N, Grinblat B et al. Markers distinguishing mesenchymal stem cells from fibroblasts are downregulated with passaging. Stem Cells Dev 2011;20:53–66.

22 Mueller MB, Tuan RS. Functional characterization of hypertrophy in chondrogenesis of human mesenchymal stem cells. Arthritis Rheum 2008;58:1377–1388.

23 Jiang Y, Chen LK, Zhu DC et al. The inductive effect of bone morphogenetic protein-4 on chondral-lineage differentiation and in situ cartilage repair. Tissue Eng Part A 2010;16:1621–1632.

24 Yin Z, Chen X, Zhu T et al. The effect of decellularized matrices on human tendon stem/progenitor cell differentiation and tendon repair. Acta Biomater 2013;9:9317–9329.

25 Song L, Webb NE, Song Y et al. Identification and functional analysis of candidate genes regulating mesenchymal stem cell self-renewal and multipotency. Stem Cells 2006;24:1707–1718.

26 Grogan SP, Chen X, Sovani S et al. Influence of cartilage extracellular matrix molecules on cell phenotype and neocartilage formation. Tissue Eng Part A 2014;20:264–274.

27 Kapoor M, Martel-Pelletier J, Lajeunesse D et al. Role of proinflammatory cytokines in the pathophysiology of osteoarthritis. Nat Rev Rheumatol 2011;7:33–42.

28 Daheshia M, Yao JQ. The interleukin 1beta pathway in the pathogenesis of osteoarthritis. J Rheumatol 2008;35:2306–2312.

29 López-Armada MJ, Caramés B, Lires-Deán M et al. Cytokines, tumor necrosis factor-alpha and interleukin-1beta, differentially regulate apoptosis in osteoarthritis cultured human chondrocytes. Osteoarthritis Cartilage 2006;14:660–669.

30 Kon E, Verdonk P, Condello V et al. Matrix-assisted autologous chondrocyte transplantation for the repair of cartilage defects of the knee: Systematic clinical data review and study quality analysis. Am J Sports Med 2009;37(suppl 1):156S–166S.

31 Tormin A, Li O, Brune JC et al. CD146 expression on primary nonhematopoietic bone marrow stem cells is correlated with in situ localization. Blood 2011;117:5067–5077.

32 Crisan M, Yap S, Casteilla L et al. A perivascular origin for mesenchymal stem cells in multiple human organs. Cell Stem Cell 2008;3:301–313.

33 Benya PD, Shaffer JD. Dedifferentiated chondrocytes reexpress the differentiated collagen phenotype when cultured in agarose gels. Cell 1982;30:215–224.

34 Diaz-Romero J, Gaillard JP, Grogan SP et al. Immunophenotypic analysis of human articular chondrocytes: Changes in surface markers associated with cell expansion in monolayer culture. J Cell Physiol 2005;202:731–742.

35 Colter DC, Class R, DiGirolamo CM et al. Rapid expansion of recycling stem cells in cultures of plastic-adherent cells from human bone marrow. Proc Natl Acad Sci USA 2000;97:3213–3218.

36 Lo T, Ho JH, Yang MH et al. Glucose reduction prevents replicative senescence and increases mitochondrial respiration in human mesenchymal stem cells. Cell Transplant 2011;20:813–825.

37 Holtzer H. Cell linages, stem cells and the "quantal" cell cycle concept. In: Lord C, Potten G, Cole G, eds. Stem Cells. Cambridge, UK: Cambridge University Press, 1978.

38 Tallheden T, Dennis JE, Lennon DP et al. Phenotypic plasticity of human articular chondrocytes. J Bone Joint Surg Am 2003;85-A(suppl 2):93–100.

39 Li L, Clevers H. Coexistence of quiescent and active adult stem cells in mammals. Science 2010;327:542–545.

40 Vasiliadis HS, Danielson B, Ljungberg M et al. Autologous chondrocyte implantation in cartilage lesions of the knee: long-term evaluation with magnetic resonance imaging and delayed gadolinium-enhanced magnetic resonance imaging technique. Am J Sports Med 2010;38:943–949.

41 Koelling S, Kruegel J, Irmer M et al. Migratory chondrogenic progenitor cells from repair tissue during the later stages of human osteoarthritis. Cell Stem Cell 2009;4:324–335.

See www.StemCellsTM.com for supporting information available online.